Chemical Science International Journal
18(3): 1-8, 2017; Article no.CSIJ.32333
Previously known as American Chemical Science Journal
ISSN: 2249-0205

SCIENCEDOMAIN *international*
www.sciencedomain.org

A Modified Poly (Trimethylene Terephthalate) Used for Fused Deposition Modeling: Synthesis and Application

Dandan Yu[1], Li Sun[1], Weilan Xue[1*] and Zuoxiang Zeng[1]

[1]Institute of Chemical Engineering, East China University of Science and Technology, 200237, Shanghai, China.

Authors' contributions

This work was carried out in collaboration between all authors. Authors DY and WX designed the study, performed the statistical analysis, wrote the protocol and wrote the first draft of the manuscript. Author LS managed the analyses of the study. Author ZZ revised the first draft of the manuscript and managed the literature searches. All authors read and approved the final manuscript.

Article Information

DOI: 10.9734/CSJI/2017/32333
Editor(s):
(1) Mohammad Luqman, Department of Basic Science, College of Applied Sciences, A'Sharqiyah University, Oman.
Reviewers:
(1) Pratima Parashar Pandey, Mangalore University, India.
(2) Leo Baldenegro, Center of Engineering and Industrial Development, Mexico.
(3) Khadiga Mohamed Abu-Zied Shaheen, University of Cairo, Egypt.
Complete Peer review History: http://www.sciencedomain.org/review-history/18388

Original Research Article

Received 21st February 2017
Accepted 20th March 2017
Published 28th March 2017

ABSTRACT

This paper presents the synthesis and application of a modified poly (trimethylene terephthalate) for Fused deposition modeling process. Five samples(S1-S5) of poly(trimethylene terephthalate-co-isophthalate-co-seacate) (PTTIS) were prepared by direct esterification and subsequent polycondensation of terephthalic acid (PTA), isophthalic acid(PIA) (n_{PTA}/n_{PIA} =7/3), sebacic acid (SA) and 1,3-propanediol (PDO) with different mole percent(α_{SA}) of SA(α_{SA}=0–4.8 mol%). The samples were characterized by gel permeation chromatography (GPC), ^{1}H-NMR spectroscopy, and differential scanning calorimetry (DSC). The mechanical properties tests showed that the tensile strength, tensile modulus, and flexural strength values of the samples increase with increasing in α_{SA} up to 1 mol%, and then decreases, while the elongation at break value the opposite, and the izod impact strength value increases with increasing in α_{SA}. The 3D printing materials which were prepared from S1-S5 were tested by a 3D printer to assess their suitability for Fused deposition

**Corresponding author: E-mail: wlxue@ecust.edu.cn;*

modeling (FDM). The results showed that the PTTIS (n_{PTA}/n_{PIA} =7/3) containing 1.0–3.8 mol% SA are suitable for FDM, and their anisotropy are better than that of ABS.

Keywords: Modified PTT; FDM; mechanical properties; 3D printing; anisotropy.

1. INTRODUCTION

The fused deposition modeling (FDM) is one of the most widely used rapid prototyping systems in the world due to its reliability, safe and simple fabrication process, and low cost of material. The FDM works as follow: the filamentous thermofusible plastic is melted, and the filament acts as a piston at the entrance of the liquefier head in FDM machine to force the molten material out of the nozzle, and then a solid three-dimensional object is obtained through the layer by layer deposition of the molten material [1]. The main use of the FDM system is to optimize the product design, short the product development cycle, reduce development costs in aerospace, home appliances, automotive, medical, military, teaching and scientific research and other fields [2]. A number of feedstock materials are available for FDM, including an investment casting wax, thermo-plastic polyester-based elastomer, poly (acrylonitrile-butadiene-styrene) (ABS) copolymer, polycarbonate, and polyphenylsulfone. However, the greatest limitation to this technology is the lack of a variety of compatible materials, because most of the above materials do not possess the strength to produce fully functional parts using FDM, limiting the applicability of parts fabricated from FDM.

There are two ways to solve this problem: synthesis of new thermoplastics possessing high strength and improvement of the properties of the existing thermoplastics. Many works have been done by the second way [3-6]. A modified ABS including liquid crystal polymer (TLCP) fibers have been used in FDM system to fabricate prototype parts, and its tensile modulus and strength were about four times those of ABS [3]. The material consisting of iron particles in a nylon type matrix material have been used successfully in the unmodified FDM system for direct rapid tooling of injection moulding inserts [4]. However, few new materials for FDM system were synthesized by the first way. Poly (trimethylene terephthalate) (PTT), a new member of the thermoplastic polyester, possesses excellent mechanical properties such as high strength, good stability and abrasion resistance [7-15]. However, it is not suitable for FDM because its melting point (~225℃) is too high. It is quite difficult to be heated to molten state for materials with high melting point in the nozzle, making FDM processing impossible.

In this paper, in order to solve the problem, PIA and SA are introduced into PTT to replace part of PTA, and five samples of poly (trimethylene terephthalate-co-isophthalate-co-seacate) PTTIS) were prepared for FDM by direct esterification and subsequent polycondensation with the constant mole ratio of PTA/PIA (n_{PTA}/n_{PIA} =7/3) and different mole percent of SA (α_{SA}=0–4.8 mol%). The samples of PTTIS were characterized by gel permeation chromatography (GPC), ^{1}H-NMR spectroscopy, and differential scanning calorimetry (DSC). The effects of the content of SA on the mechanical properties of PTTIS were investigated. And the suitability of the 3D printing materials prepared from the samples were tested by a 3D printer.

2. MATERIALS

Terephthalic acid (PTA), isophthalic acid (PIA), and sebacic acid (SA) were purchased from Shanghai Yetan Chemical Industry Co., Ltd (China), and 1,3-propanediol (1,3-PDO) was provided by Shanghai Haiyu Chemical Industry Co., Ltd(China). Tetrabutoxytitanium ($Ti(OBU)_4$) was obtained from tetrabutyl titanate Shanghai Chemistry Reagent Company (China). Talc powder was provided by Shanghai huanyu Chemical co. Ltd(China). 2,5-dihexadecylhexanediamide was obtained from Shanghai Huayi Chemical Auxiliary Co., Ltd (China). Antioxygen 1076 was purchased from Zibo Xiangdong Chemical Co., Ltd (China).

2.1 Preparation of PTTIS

In this paper, five samples(S1,S2,S3,S4,and S5) of PTTIS were prepared by direct esterification and subsequent polycondensation from PTA, PIA, SA and 1,3-PDO, in the presence of $Ti(OBU)_4$ as catalyst. Formulas for the preparation of PTTIS are shown in Table 1. The detailed preparation program was similar to that in elsewhere [16], and it was described briefly as follows: The mixture of TPA, PIA, SA, 1,3-PDO, and $Ti(OBU)_4$

Table 1. Formulas for the preparation of PTTIS

Sample	Feed[a](mol%)		Copolyester composition[b] (mol%)	
	$n_{PTA}+n_{PIA}$ (n_{PTA}/n_{PIA})=7/3	SA	$n_{PTA}+n_{PIA}$ (n_{PTA}/n_{PIA})=7/3	SA
S1	100	0	100	0
S2	99	1	98.98	1.02
S3	97.6	2.4	97.57	2.43
S4	96.2	3.8	96.21	3.79
S5	95.2	4.8	95.19	4.81

[a]Molar percent of PTA, PIA and SA fed in the polymerization
[b]Measured by ^{1}H-NMR spectroscopy

was put into a three-necked round-bottom flask equipped with a mechanical stirrer and a distillation column, and was continuously stirred and kept in the range of 170–215℃ until the solution becomes transparent. After esterification, the mixture was heated up to 255℃ and kept for 2 h for polycondensation with reduced pressure (60-80Pa), thus the sample of PTTIS with various sebacic acid content could be prepared.

3. CHARACTERIZATION

3.1 Gel Permeation Chromatography (GPC)

The molecular weights (Mw, Mn) of the samples were determined by GPC (Waters 1515, USA) with refractormeter 2414 as a detector at 25℃, using hexafluoroisopropanol as a solvent.

3.2 ^{1}H -NMR

The chemical compositions of the samples were analyzed by means of ^{1}H-NMR spectra (500 MHz NMR, Varian, MERCURY plus 400) using the mixture of $CDCl_3$/CF_3COOD as a solvent.

3.3 Differential Scanning Calorimetry (DSC)

The glass transition temperature (Tg), the temperature of crystallizing peak (Tc) and the melting temperature (Tm) of the samples were determined by using a differential scanning calorimeter instrument (DSC1, METTLER TOLEDO, Switzerland) under a nitrogen atmosphere. The sample was first heated from 10℃ to 220℃ at a heating rate of 10℃/min and maintained at 220℃ for 5 minutes to erase the thermal history. The sample was cooled down to -10℃ at a cooling rate of 70℃/min, and then heated again to 220℃at the heating rate of 10℃/min. The second heating curves were analyzed to obtain the value of T_g , T_c and T_m.

3.4 Viscosity Testing

The melt viscosity of samples were measured using a Brookfield viscometer (DV-11 Pro) with a spindle (SC4-27) rotating at 15 rpm from 210℃ to 230℃.

3.5 Mechanical Property

3.5.1 Tensile properties

The specimens of the sample were tensile-tested in a Universal Testing Machine (SHIMADZU, AGS-X 500 N, Japan) equipped with extensometer at the room temperature according to ASTM D 638 standard. All the tests were performed with the cross-head speed of 50 mm/min .Three specimens were tested in each case, and the average value was recorded.

3.5.2 Izod impact properties

The specimens of the sample were impact-tested in a cantilever beam impact testing machine according to GB/T1043-1992. All the tests were performed at a constant impact velocity of 3.5 m/s. Six specimens were tested in each case, and the average value was recorded.

3.5.3 Flexural properties

The specimens of the sample were bend-tested in a bend testing machine (PT-307, Precise Test, Dongguan, China). The 2.5 kN load cell was applied for the measurements at a constant cross head speed of 1 mm/min. The mechanical testing was stopped when specimen was fractured. ten specimens were tested in each case, and the average value was recorded.

4. RESULTS AND DISCUSSION

4.1 The Molecular Weight and Chemical Composition of Pttis

The molecular weights of S1-S5 determined by GPC were shown in Table 2. From Table 2, these samples have a similar range of molecular weights (Mn= 72900 - 74900 Da). The ^{1}H-NMR spectra of S1-S5 were measured and that of S3 was illustrated in Fig. 1. From Fig. 1, S3 shows the characteristic peaks at 7.83(a), 8.23(g), and 1.28 ppm (f), which are attributed to protons of PTA, PIA and SA, respectively. The molar ratio of the PTA, PIA, and SA units on the polymer backbone was calculated from integrations of their specific chemical shifts. The results are summarized in Table 1. The composition data in Table 1 indicates that almost all the PTA, PIA, and SA fed in the polymerization come into the resultant polymer.

Table 2. Molecular weight and distribution

Sample	Mw(Da)	Mn(Da)	Mw/Mn
S1	84600	73500	1.15
S2	86500	73900	1.17
S3	89200	74900	1.19
S4	87500	72900	1.20
S5	91300	74200	1.23

4.2 Thermal Properties of PTTIS

Thermal properties of S1-S5 were measured by the procedure described in the above, and one of the DSC thermograms (S3) is shown in Fig. 2. From the DSC thermograms, the values of T_g, T_c and T_m for the samples can be obtained and shown in Table 3. As we can seen from Table 3, the T_g values of PTTIS increases from 43.4ºC to 45.9ºC with increasing in α_{SA} up to 1 mol%, and then decreases from 45.9ºC to 35.6ºC. Similarly, the T_m values of PTTIS increases from 182.8ºC to 183.9ºC with increasing in α_{SA} up to 1mol%, and then decreases from 183.4ºC to 175.3ºC. While the T_c value the opposite. The above phenomenon may be caused by the changes of crystalline properties of PTTIS. SA may play two roles in the crystallization of PTTIS: (1) it acts as a longer chain to facilitate crystallization and (2) as a third component disturbs the regularity of the co-polymer mocecular chain to retard crystallization [17-19]. Therefore, from the above data, we could speculate that SA (α_{SA}≤1 mol%) can accelerate crystallization of PTTIS, and a lot of microcrystal can be formed in a short time to play a role similar to the "physical cross-linking point", which limits the movement of the chain segments in the non crystalline part [20] and then leads to the increase of T_g and T_m. However, the later will play its role when α_{SA} is greater than or equal to 2.4 mol%.

4.3 Mechanical Properties of PTTIS

Based on the method described in the above, the results of tensile strength at peak, elongation at break, izod impact strength and flexural strength for S1-S5 were presented in Fig. 3. From Fig. 3, the tensile strength and flexural strength values of PTTIS increase with increasing in α_{SA} up to 1 mol%, and then decrease, while the elongation

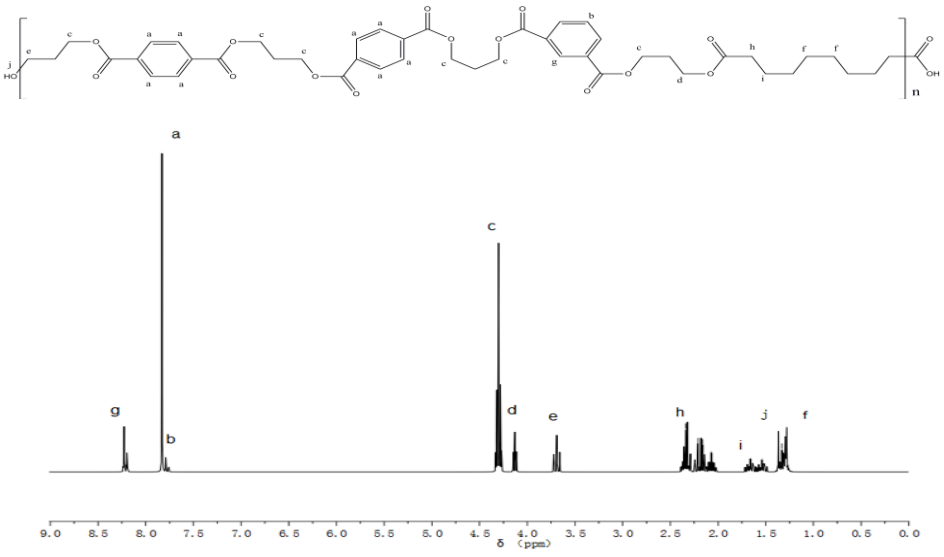

Fig. 1. The ^{1}H-NMR spectra of S3

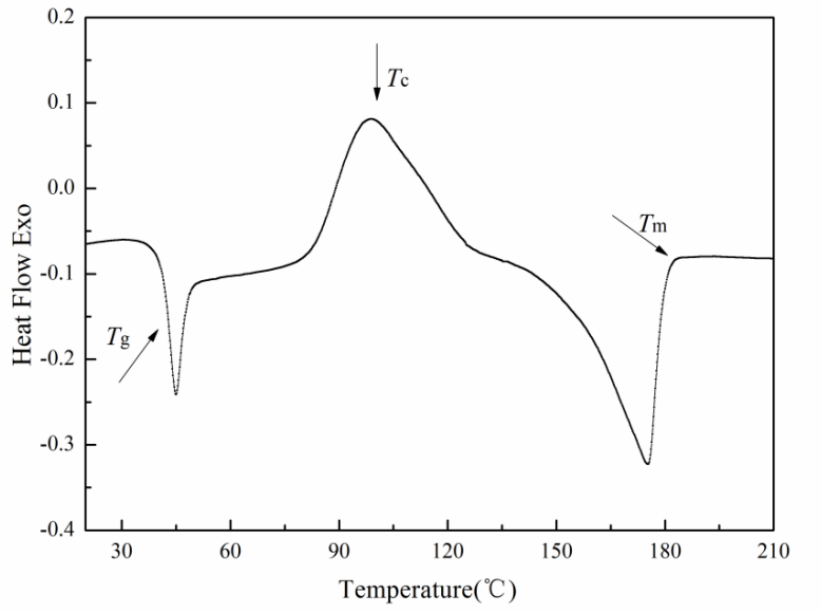

Fig. 2. DSC thermograms of S3

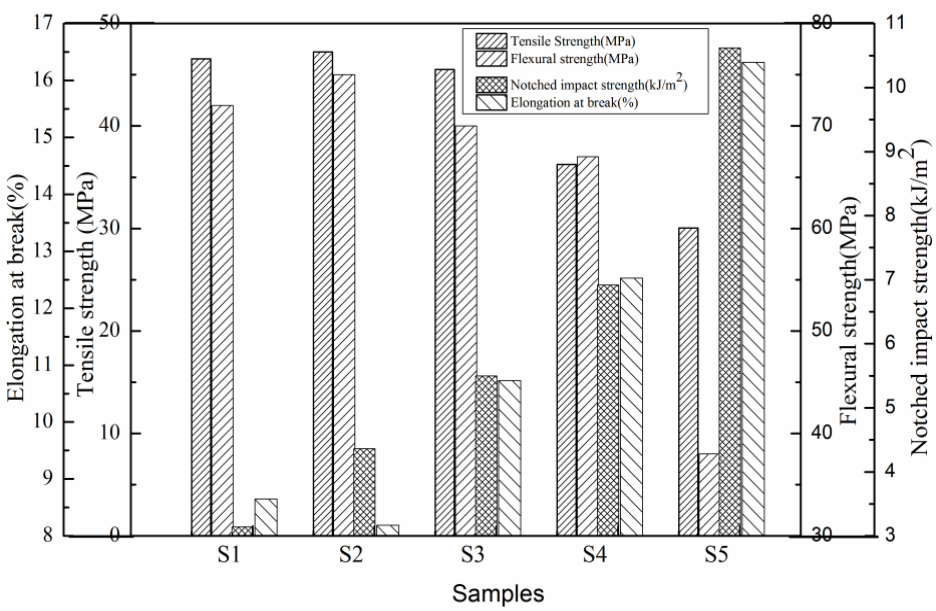

Fig. 3. The values of tensile strength, flexural strength, izod impact strength and elongation at break

at break value the opposite. These results may be also induced by the effect of SA on the crystalline properties of PTTIS.

On the other hand, the izod impact strength value increases with increasing in α_{SA}, indicating both the formation of microcrystal (α_{SA}≤1 mol%) and the disturbances of the regularity of the mocecular chain(α_{SA}≥2.4mol%) are helpful to enhance the izod impact strength.

4.4 Rheological Properties of PTTIS

The melt viscosity values (η) of S1- S5 were measured from 210-230ºC by the procedure described above, and the results were shown in Table 4. From Table 4, the viscosities of S2-S5 are one order of magnitude smaller than that of S1, indicating the introduction of SA is beneficial to successful printing in FDM. The temperature dependency of viscosity is a factor

that should be considered for the practical utilization of the PTTIS, because low viscosity at the time of application is a desirable attribute for its ability to be processed. The relationship between η and the activation energy for flow (E) can be expressed by Equation (1) and (2)

$$\eta = \eta_0 \exp(E / RT) \quad (1)$$

$$\ln \eta = E / RT + \ln \eta_0 \quad (2)$$

where R is the gas constant and η_0 is the pre-exponential factor. The plots of ln(η) versus 1/T for the samples shown in Fig. 4 are approximately linear. The E values for these samples are listed in Table 4.

Table 3. The values of T_g, T_c and T_m

Sample	T_g (ºC)	T_c (ºC)	T_m(ºC)
S1	43.4	114	182.8
S2	45.9	107	183.9
S3	41.8	115	181.0
S4	40.3	118	178.6
S5	35.6	119	175.3

4.5 Fabrication of Filaments for FDM Processing

The feedstock filaments need to be of specific size, strength and properties for successful FDM processing. In order to create such filaments from S1-S5, a desktop wiredrawing extruder (HXY-ZS, CHINA) equipped with a die diameter of 3.6 mm was used. The polymer powder of S1-S5 containing talc powder as additive (1 wt%), 2,5-dihexadecylhexanediamide as lubricant (0.5 wt%) and antioxygen 1076 (0.5 wt%) was added to the feed hopper, and the powder material flows into the extruder barrel from the feed hopper by gravity.

Table 4. The melt viscosity values

Sample	Melt viscosity(Pa·s)			E (kJ)
	210℃	220℃	230℃	
S1	1234	862	587	77.22
S2	174	112	78	83.35
S3	164	97	62	101.12
S4	163	102	73	83.56
S5	115	65	45	115.04

During the extrusion process, die swell phenomenon occurs, and the molten material will swell when coming out of the die [21]. Because of swelling, the diameter of the filament will be bigger than that of the die. On the other hand, when the traction speed is bigger than the extrusion speed, the diameter of the filament will become smaller. Furthermore, the extrusion speed is related with the temperature of extruder barrel. In this work, the temperature of barrel heaters is generally 20℃ lower than the melting point of the composite. Since the barrel is stationary and the screw is rotating, the frictional forces will act on the material. As the material moves forward, it will heat up as result of frictional heat generated and conducted from generated and conducted from the barrel heaters. When the temperature of the material exceeds the melting point, the melted material is simply pumped to the die. By adjusting extrusion speed and traction speed, the filaments with desired diameter are produced. After repeated test, uniform filaments have been made from S1-S5.

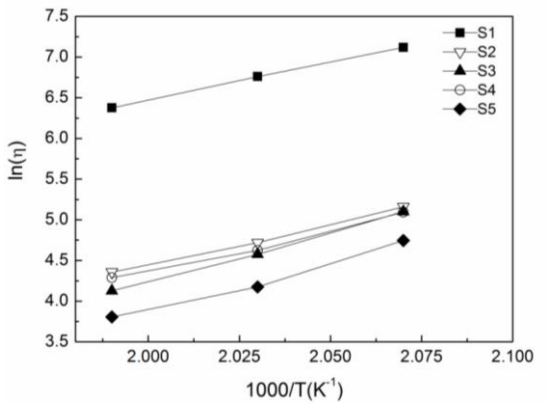

Fig 4. The plots of ln(η) versus 1/T

4.6 Printing Process

The feedstock filaments made from S1-S5 were loaded into spool of a FDM machine (Panowin F3Cl, Φ3mm, CHINA) and were fed into the nozzle for part fabrication. The results showed that the filaments made from S2- S4 can be printed fluently in the FDM machine in the temperature range of 210-230ºC. However, the filaments made from S1 and S5 cannot be used to print parts due to nozzle clogging. The reasons for nozzle clogging may be the viscosity is too large (S1) or the bending strength is too low (S5). According to the data in Fig. 3 and Table 4, the ratios (β) of bending strength to viscosity for S1-S5 at 210-230ºC are listed in Table 5. From Table 5, the β values for S2-S4 are higher than that for S1 and S5 at the same temperature.

Table 5. The ratios (β) of bending strength to viscosity for S1-S5 at 210-230℃

Sample	β		
	210℃	220℃	230℃
S1	0.06	0.08	0.12
S2	0.43	0.67	0.96
S3	0.43	0.72	1.13
S4	0.41	0.66	0.92
S5	0.33	0.58	0.84

4.6.1 The anisotropy of UTS and elongation at break values for S2, S3 and S4

Like other 3D printing methods, parts fabricated from FDM will exhibit physical property anisotropy. In most cases, the analysis of ultimate tensile strength can be used to observe the mechanical property anisotropy. For this reason, two sets of specimens were produced, one printed in the XYZ direction and the other printed in the ZXY direction (as shown in Fig. 5) for each material type, and the percent difference (Δ_{UTS} and Δ_{EL} the difference in UTS values relative to the horizontally printed samples) was used to characterize the mechanical property anisotropy of the materials as follow:

$$\Delta_{UTS} = \frac{UTS_{(XYZ)} - UTS_{(ZXY)}}{UTS_{(XYZ)}} \times 100\% \quad (1)$$

$$\Delta_{EL} = \frac{EL_{(XYZ)} - EL_{(ZXY)}}{EL_{(XYZ)}} \times 100\% \quad (2)$$

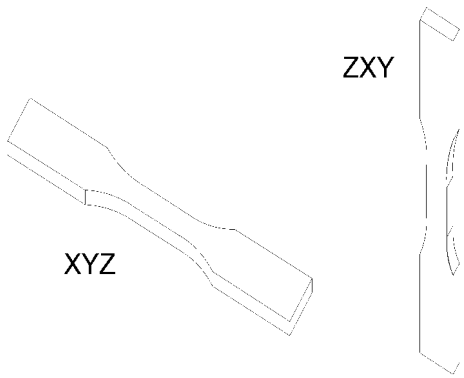

Fig. 5. Specimens printed in the XYZ (horizontal) and ZXY (vertical) directions

Table 6 presented tensile test results of specimens built in different orientations. From Table 6, we obtain that the values of Δ_{UTS} (23.2 – 26.7%) and Δ_{EL} (37.839.6%) for the modified PTT are lower than that for ABS (Δ_{UTS}=47.79% and Δ_{EL}=75.92%,respectively)[22].

Table 6. Tensile test results of specimens built in different orientations

Samples	UTS(MPa)			EL (%)		
	XYZ	ZXY	Δ_{UTS} (%)	XYZ	ZXY	Δ_{EL} (%)
S2	47.22	36.26	23.2	8.19	5.13	37.8
S3	45.52	34.37	24.5	10.73	6.62	38.3
S4	36.25	26.57	26.7	12.53	7.57	39.6

5. CONCLUSIONS

The samples of PTTIS were prepared by introducing PIA (n_{PTA}/n_{PIA} =7/3) and SA (α_{SA}=0–4.8 mol%) into PTT to replace part of PTA. The effects of α_{SA} on the mechanical properties of PTTIS were investigated, and the results showed that the tensile strength, tensile modulus, and flexural strength values of PTTIS increase with increasing in α_{SA} up to 1 mol%, and then decreases, while the elongation at break value the opposite, and the izod impact strength value increases with increasing in α_{SA}. The 3D printing materials which were prepared from S1-S5 were tested by a 3D printer and the results showed that the PTTIS (n_{PTA}/n_{PIA} =7/3) with α_{SA} = 1.0–3.8 mol% display desirable mechanical properties, and flexible filaments of S2-S4 can be printed fluently in the FDM machine.

COMPETING INTERESTS

Authors have declared that no competing interests exist.

REFERENCES

1. Yu DM. Process analysis and application for rapid prototyping based on fused deposition modeling. Mach Design Manuf. 2011;8:65-67. (in Chinese).
2. Chulilla Cano JL. the cambrian explosion of popular 3D printing. IJIMAI. 2011;4:30-31.
3. Gray RW, Baird DG, Jan Helge Bohn. Effects of processing conditions on short TLCP fiber reinforced FDM parts. Rapid Prototyp J. 1998;4:14–25.
4. Masood SH, Song WQ. Development of new metal/polymer materials for rapid tooling using Fused deposition modeling. Mater Design. 2004;25;587–594.

5. Shofner ML, Lozano K, Rodríguez-Macías FJ, Barrera EV. Nanofiber-reinforced polymers prepared by fused deposition modeling. J Appl Polym Sci. 2003;89: 3081–3090.
6. Nikzad M, Masood SH, Sbarski I. Thermo-mechanical properties of a highly filled polymeric composites for fused deposition modeling. Mater Design. 2011;32:3448–3456.
7. Wu T, Li Y, Wu Q, Song L, Wu G. Thermal analysis of the melting process of Poly (trimethylene terephthalate) using FTIR micro-spectroscopy. Eur Polym J. 2005;41: 2216-2223.
8. Chen KQ, Tang XZ, Shen J, Zhou Y, Zhang B. Non-isothermal crystallization behavior of poly(trimethylene terephthalate) synthesized with different catalysts. Macromol Mater Eng. 2004;289:539-547.
9. Sumod Kalakkunnath, Douglass S. Kalika. Dynamic mechanical and dielectric relaxation characteristics of poly (trimethylene terephthalate). Polym. 2006; 47:7085-7094.
10. Hoe H. Chuah. Orientation and structure development in poly (trimethylene terephthalate) tensile drawing. Macromolecules. 2001;34:6985-6993.
11. Bojie Wang, Christopher Y. Li, Jennifer Z. D. Cheng, Phillip H. Geil, Janusz Grebowicz, Rong-Ming Ho. Poly (trimethylene terephthalate) crystal structure and morphology in different length scales. Polym. 2001;42:7171-7180.
12. Kurian JV. A new polymer platform for the future-sorona from com derived 1,3-propanediol. J Polym Environ. 2005;13: 159-167.
13. Xu Y, Jia HB, Ye SR, Huang J. Synthesis and crystallization behavior of poly (trimethylene terephthalate) poly (ethylene glycol) segmented copolyesters. J Mater Sci. 2007;42:8381-8385.
14. Jakeways R, Ward IM, Wilding MA, Hall IH, Desborough IJ, Pass MG. Crystal deformation in aromatic polyesters. J Polym Sci Polym Phys Ed. 1975;13:799-813.
15. Ward IM, Wilding MA, Brody H. mechanical-properties and structure of poly (meta-methylene terephthalate) fibers. J Polym Sci Polym Phys Ed. 1976;14:263-274.
16. Zhu WP, Gou PF. Synthesis, extraction, and adsorption properties of Calix [4]arene-poly(ethylene-glycol) Crosslinked Polymer. J Appl Polym Sci. 2008;109: 1968–1973.
17. Zou HT, Li G. Characterization and crystallization behavior of poly (ethylene-co-trimethylene-terephthalate) Copolymers. Polym Eng Sci. 2008;10:511-518.
18. George ZP, Stavroula GN. Synthesis and characterization of novel poly (propylene terephthalate-co-adipate) biodegradable random copolyesters. Polym Degrad Stabil. 2010;95:627-637.
19. Zou HT, Li G. Characterization and crystallization behavior of poly (ethylene-co-trimethylene-terephthalate) copolymers. Polym Eng Sci. 2008;10:511-518.
20. Liu YX, An J, Sun QY. Study on crystallization behavior of PET copolyester. Polym Mater Sci Eng. 1994;4:79-84 (in Chinese).
21. Rauwendaal C. Polymer extrusion. Munich: Hanser Publishers; 2001.
22. Torrado AR, Shemelya CM, Wicker RB, Characterizing the effect of additives to ABS on the mechanical property anisotropy of specimens fabricated by material extrusion 3D printing, Additive Manufacturing. 2015;6:16-29.

Peer-review history:
The peer review history for this paper can be accessed here:
http://sciencedomain.org/review-history/18388